JOURNAL OF MATERIALS SCIENCE 23 (1988) 509–514

Density and deposition rate of chemical-vapour-deposited boron nitride

TOSHITSUGU MATSUDA
Japan Metals and Chemicals Co., Ltd, 1719 Ohmama, Yamada-gun, Gunma 376-01, Japan
HIROYUKI NAKAE
The Furukawa Electric Co., Ltd, 9-15 Futaba 2-chome, Shinagawa-ku, Tokyo 142, Japan
TOSHIO HIRAI
The Research Institute for Iron, Steel and Other Metals, Tohoku University, Sendai 980, Japan

A study is made on the density and deposition rate characteristics of chemical-vapour-deposited boron nitride (CVD-BN) plates synthesized by use of the BCl_3–NH_3–H_2 system at a deposition temperature (T_{dep}) of 1200 to 2000° C and a total gas pressure (P_{tot}) of 5 to 60 torr. At a P_{tot} of 5 torr, all the CVD-BN plates synthesized at each T_{dep} above 1300° C had a density greater than 2.0 g cm^{-3}, and thus showed no noticeable dependence on T_{dep}. Over the P_{tot} range from 10 to 60 torr, on the other hand, the density of the plates reached the maximum of 2.08 g cm^{-3} at a T_{dep} of 2000° C. As T_{dep} was lowered, the density decreased down to a minimum of 1.40 g cm^{-3}. The deposition rate varied with both T_{dep} and P_{tot}, and showed a maximum value under a certain P_{tot} at a given T_{dep}. The value of P_{tot} where the deposition rate becomes maximum changed depending on the T_{dep}. The maximum deposition rate was 0.6 mm h^{-1} for the CVD-BN plates when the density was less than 2.0 g cm^{-3}, and 0.4 mm h^{-1} when the density was above 2.0 g cm^{-3}. The effects of deposition conditions on the characteristics of density and deposition rate are discussed in terms of the structure and deposition mechanism.

1. Introduction

The method of chemical vapour deposition (CVD) is a well-known technique for coating and producing thin films. However, the CVD method has recently become recognized as an effective method in producing a free-standing body with high chemical purity and high density from materials which are not easily sintered, such as nitride and carbide. In producing free-standing bodies by the CVD method a rapid deposition rate was attained by controlling the gas flow pattern. For example, free-standing bodies of CVD-Si_3N_4 with a thickness of 4 to 5 mm were obtained under a maximum deposition rate of 1.2 mm h^{-1} [1].

Much attention has been paid recently to obtaining a high deposition rate of CVD-BN because free-standing bodies of CVD-BN are useful as crucibles for the growing of GaAs and as structural materials for equipment in the field of semiconductors.

Most studies on the synthesis of CVD-BN in the past have concentrated on processes using the B_2H_6–NH_3 and BCl_3–NH_3 systems. The former has been utilized for manufacturing thin films while the latter is used for producing free-standing bodies as well as thick films. For CVD-BN thin-film synthesis with the B_2H_6–NH_3 system, the effects of deposition conditions on properties and deposition rate have been investigated in detail [2–9]. However, in the production of free-standing bodies by use of the BCl_3–NH_3 system there is little information available for a similar relationship between the deposition conditions and the product properties and deposition rate of CVD-BN.

The present authors have previously reported results on the structures of CVD-BN plates prepared under various deposition conditions by using the BCl_3–NH_3–H_2 system [10]. The present paper describes the results of a study concerning the effects of deposition temperature and total gas pressure on the density and deposition rate of CVD-BN plates.

2. Experimental procedure

2.1. Synthesis of CVD-BN plate

BCl_3, NH_3 and H_2 gases were used to synthesize CVD-BN plate (about 30 mm × 10 mm × 0.2 to 1 mm) on a graphite substrate which was heated directly by an electric current. Details of the synthesis procedure have been described in the previous paper [10]. The deposition conditions are summarized in Table I. CVD-BN plates having various structures were obtained depending on the deposition temperature (T_{dep}) and the total gas pressure (P_{tot}), as shown in Fig. 1 [10]. CVD-BN plates obtained in the A and B regions in Fig. 1 were transparent turbostratic BN (t-BN) [11] with isotropic properties and semi-transparent t-BN with anisotropic properties, respectively. In the C region, a mixture of two kinds of t-BN having different interlayer spacings ($c_0/2$) was deposited. This CVD-BN plate was either semi-transparent or white opaque material and was denoted

0022–2461/88 $03.00 + .12

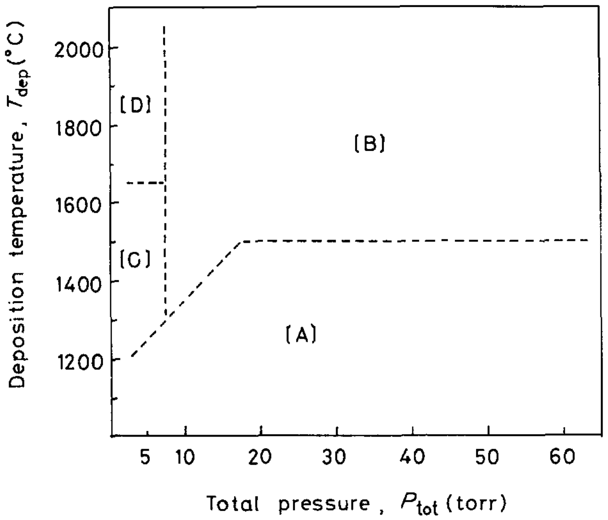

Figure 1 Effects of T_{dep} and P_{tot} on the crystal structure of CVD-BN plate [10]. Type A, isotropic t-BN (turbostratic BN); Type B, anisotropic t-BN; Type C, a mixture of two kinds of t-BN different in $c_0/2$ ((t + t′)-BN, where t′ denotes t-BN with a smaller $c_0/2$); Type D, a mixture of t-BN and h-BN ((t + h)-BN, where h denotes hexagonal BN).

as (t + t′)-BN, where t-BN with a smaller $c_0/2$ was denoted as t′-BN in order to distinguish it from the t-BN with a larger $c_0/2$. The deposit obtained in the D region was a white opaque plate composed of t-BN and hexagonal BN (h-BN) (denoted as (t + h)-BN). Both (t + t′)-BN and (t + h)-BN were anisotropic plates. CVD-BN plates synthesized under the conditions shown in Table I were subjected to measurements of their density and deposition rate in this work.

2.2. Density of CVD-BN plate

CVD-BN plate formed on a graphite substrate was removed from the substrate, and the small amount of graphite remaining on the CVD-BN plate was completely removed using emery paper (Nos 800 and 1500). The bulk density of CVD-BN plate (about 30 mm (or 10 mm) × 10 mm × 0.2 to 1 mm) was measured by the Archimedean method using toluene. The specific gravity of toluene was corrected for the proper temperature.

2.3. Deposition rate of CVD-BN plate

The weight of CVD-BN plate (W mg) was determined by subtracting the weight of the substrate from the weight of the original deposit and substrate. As seen from Fig. 2, the weight of CVD-BN plate increased linearly with the deposition time. Accordingly, the deposition rate constant (K mg mm^{-2} h^{-1}) is calculated from the relationship $K = (W/S)/t$, where S and t are the surface area of the substrate (mm^2) and the deposition time (h), respectively. In addition, the average rate of increase in thickness (L mm h^{-1}) was calculated from the following equation in terms of K and the density of the plate (ϱ g cm^{-3}): $L = K/\varrho$. For some CVD-BN plates, the thickness was determined by averaging the ten values measured across the cross-section using a travelling microscope and then calculating the rate of increase in thickness. The rate obtained from thickness measurements agreed closely with the L value calculated from the above equation.

TABLE I The preparation conditions of CVD-BN plate

Deposition temperature, T_{dep} (°C)	1200 to 2000
Total gas pressure, P_{tot} (torr)	5 to 60
Gas flow rate, (cm^3 min^{-1})	
NH_3	90
BCl_3	140
H_2	670
Deposition time, t (h)	1 to 9

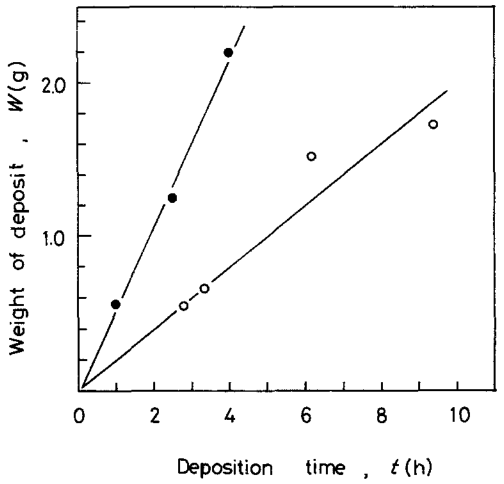

Figure 2 Time dependence of weight increase of CVD-BN plate at P_{tot} = 10 torr and T_{dep} = (○) 1400, (●) 1800°C.

Under a P_{tot} of 60 torr, the thickness varied along the gas stream path as reported in the previous paper [10]. For example, the CVD-BN plate obtained at 60 torr and 1600° C had a thickness at the end part of the plate under the upper stream of source gases of about 2.7 times that of the centre portion of the CVD-BN plate. Although the L values of the CVD-BN plate formed at 60 torr are not good representations for actual shapes of the plates, they are included in Fig. 5 as reference data to be compared with the results obtained under other preparation conditions.

3. Results

3.1. Bulk density

Fig. 3 shows the effect of total gas pressure (P_{tot}) on the density of CVD-BN plate. As shown in Fig. 3, the CVD-BN plate obtained at 5 torr had the highest

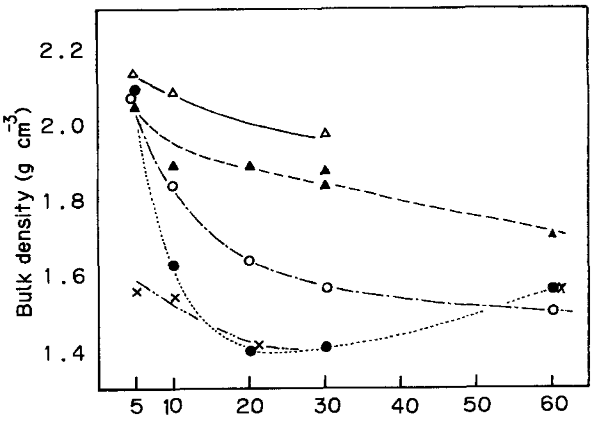

Figure 3 Effect of P_{tot} on the bulk density of CVD-BN plate. T_{dep} = (x) 1200, (●) 1400, (○) 1600, (▲) 1800, (△) 2000°C.

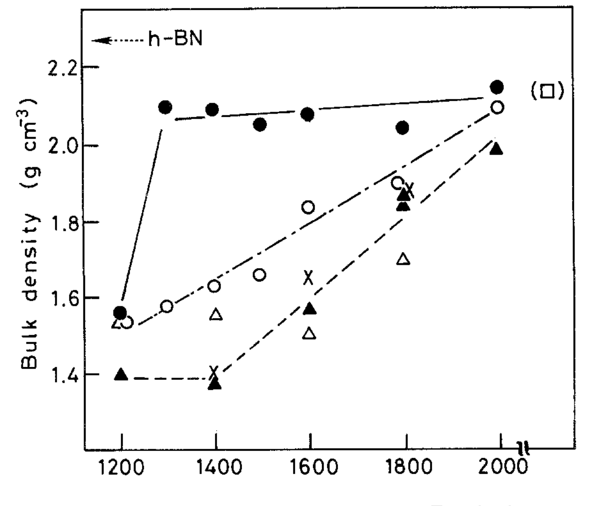

Figure 4 Effect of T_{dep} on the bulk density of CVD-BN plate. (□) Commercially obtainable CVD-BN (Union Carbide Corp.). P_{tot} = (●) 5, (○) 10, (x) 20, (▲) 30, (△) 60 torr.

density, and the density of CVD-BN plate was decreased as P_{tot} increased. The rate of density change is remarkable at the lower deposition temperatures (T_{dep}).

The effect of T_{dep} on the density is shown in Fig. 4. It can be seen from Fig. 4 that above T_{dep} = 1300° C the CVD-BN plate synthesized at 5 torr has a density of more than 2.0 g cm^{-3}, almost independent of T_{dep}. As reported in the previous paper [10], the CVD-BN plate obtained at 5 torr (C and D regions in Fig. 1) was a mixture of two kinds of BN with different interlayer spacings ($c_0/2$). On the other hand the CVD-BN plates prepared at above 10 torr (A and B regions in Fig. 1) consisted solely of turbostratic BN (t-BN) [10], and had a lower density at a lower T_{dep}.

In the present study, the density of CVD-BN plate reached a maximum of 2.14 g cm^{-3} at 2000° C and 5 torr, where *t*-BN and h-BN were co-deposited. The t-BN plates deposited in the A region in Fig. 1 were transparent, isotropic and glassy, having a low density. The minimum density for CVD-BN plate measured in this work was 1.40 g cm^{-3}. This value was obtained for the sample produced at 1200 to 1400° C and 20 to 30 torr in the A region. Theoretically, h-BN has been reported to have a density of 2.27 g cm^{-3} [12]. The bulk densities of the CVD-BN plates obtained in this work correspond to 62 to 94% of the theoretical values.

3.2. Deposition rate

Changes in the rate of increase of thickness for CVD-BN plate with P_{tot} are illustrated in Fig. 5. As can be seen in Fig. 5, the maximum rate of increase in thickness was 0.6 mm h^{-1} and was obtained at 30 torr and 1600° C. This CVD-BN plate had a density of 1.6 g cm^{-3} and consisted of t-BN. Higher-density plates of above 2.0 g cm^{-3} were deposited with a rate of 0.4 mm h^{-1} at 2000° C and 10 torr. CVD-BN plate having a similar structure (mixture of t-BN and h-BN) and density (greater than 2.1 g cm^{-3}) to those of the commercially available CVD-BN free-standing body was obtained in the D region and its highest rate of increase in thickness was found to be 0.17 mm h^{-1}.

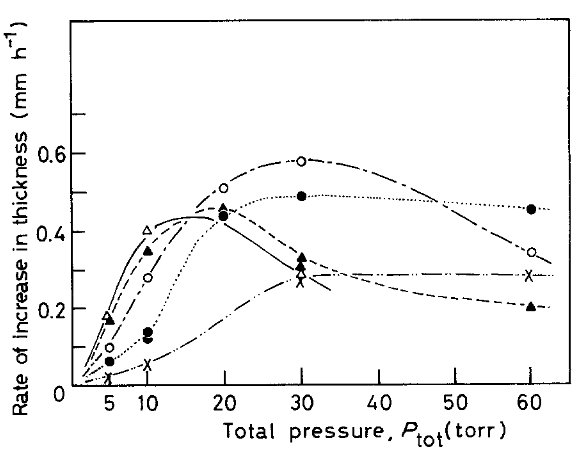

Figure 5 Effect of P_{tot} on the rate of increase in thickness of CVD-BN plate. T_{dep} = (x) 1200, (●) 1400, (○) 1600, (▲) 1800, (△) 2000° C.

Fig. 6 shows the effect of P_{tot} on the deposition rate constant (K) of CVD-BN plate. The deposition rate constant initially increased with increase in P_{tot} until it reached the maximum at a certain P_{tot}. It is also seen that the P_{tot} value which gives a maximum deposition rate constant at a given T_{dep} is larger for a lower T_{dep}.

Fig. 7 shows an Arrhenius plot of the deposition rate constant against the reciprocal of T_{dep} under various pressures P_{tot}. The values observed at P_{tot} = 20 to 60 torr have a definite maximum. In these curves, the value of T_{dep} at which a maximum occur changes depending on P_{tot}; for example, the maximum deposition rate constant at higher P_{tot} values is found at lower values of T_{dep}. At P_{tot} = 5 and 10 torr, linear relations are observed for temperatures below 1400° C. From the gradients of these linear portions, the activation energy of CVD-BN formation was calculated to be 32 kcal mol^{-1} (134 kJ mol^{-1}).

4. Discussion

4.1. Density of CVD-BN plate

Basche [13] reported that his experiments showed densities of 1.99 to 2.20 g cm^{-3} at deposition temperature of 1850 to 2200° C and 1.45 g cm^{-3} at 1450° C for CVD-BN synthesized by using the BCl_3–NH_3 system. Archer [14] mentioned in his review that CVD-BN

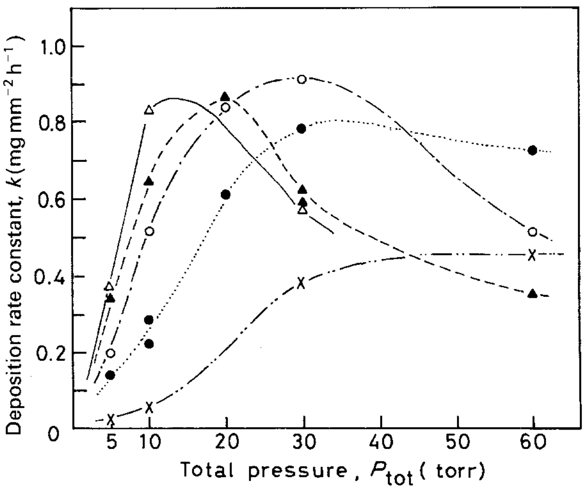

Figure 6 Effect of P_{tot} on the deposition rate constant of CVD-BN plate. T_{dep} = (x) 1200, (●) 1400, (○) 1600, (▲) 1800, (△) 2000° C.

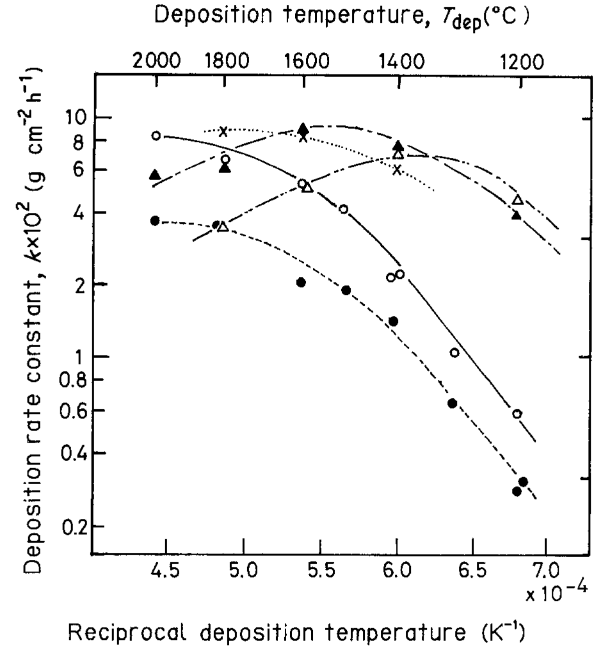

Figure 7 Arrhenius plot of the deposition rate constant of CVD-BN plate. P_{tot} = (●) 5, (○) 10, (x) 20, (▲) 30, (△) 60 torr.

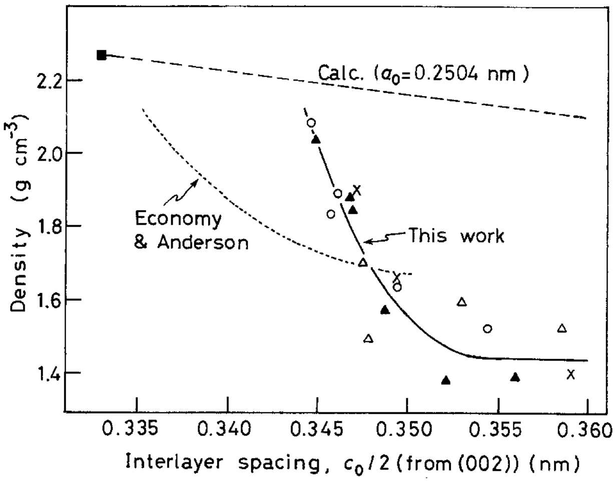

Figure 8 Correlation between density and interlayer spacing of CVD-BN plate. P_{tot} = (○) 10, (x) 20, (▲) 30, (△) 60 torr.

prepared at 1820 to 1920° C by using the BX_3–NH_3 system had a density of 1.85 to 2.05 g cm^{-3}, and Pierson [15] referred to the observation that CVD-BN prepared at 1200° C by using the BCl_3–NH_3 system had a density of 1.42 g cm^{-3}. These values of the densities are consistent with the results of the present work. However, there seems to be no known work which studied the density change in terms of the deposition conditions, or which reveals the relationship between the density and structure of CVD-BN plate. The present work has clearly demonstrated that various CVD-BN plates with densities in the range 1.40 to 2.14 g cm^{-3} are obtainable by proper control of the deposition conditions, and furthermore it was shown that the application of a different P_{tot} will result in a different density at the same T_{dep} (Fig. 3). The finding that even at a low T_{dep} of 1300° C the resulting deposit can have a high density of greater than 2.0 g cm^{-3} when the applied pressure is below 5 torr has never been reported prior to this work, and is to be noted. The two different T_{dep} dependences of density for the deposits formed at 5 torr and above 10 torr (Fig. 4) may be related to the deposition mechanisms of these CVD-BN plates as will be discussed later.

Economy and Anderson [16] synthesized BN fibre by reducing and nitriding boron oxide with ammonia and examined the relationship between the interlayer spacing of the c plane ($c_0/2$) and the density of the BN fibre. Fig. 8 compares their results (dotted line) with those obtained in the present work (solid line). No data for the CVD-BN plate obtained at 5 torr are plotted in Fig. 8 because the data contain two kinds of BN having different value of $c_0/2$. The theoretical value of the density for hexagonal BN can be calculated based on its lattice constants as 2.27 g cm^{-3}. However, BN plate prepared by the CVD method mainly consists of t-BN with a larger $c_0/2$. A density change corresponding to such a large $c_0/2$ (from (0 0 2)) was calculated under the assumption that the value of a_0 of 0.2540 nm reported by Pease [12] remains valid [17], and the results are shown as a dashed line in Fig. 8. The difference between the calculated and measured densities is due to the existence of internal pores. Thus, Fig. 8 suggests that the CVD-BN plate composed of BN crystallites with a larger $c_0/2$ contains a large number of internal pores. Our results agreed with those of Economy and Anderson [16] at relatively large $c_0/2$ (about 0.35 nm). A larger difference between Economy and Anderson's results and the calculated theoretical density at smaller $c_0/2$ than the corresponding difference for the present work suggests that the CVD-BN plate obtained in this study appeared to contain a smaller number of internal pores than the BN fibre of Economy and Anderson at a small $c_0/2$. It can be concluded from these findings that $c_0/2$ is not the only factor that determines the bulk density of CVD-BN plate. The BN fibre was reported to be isotropic [16], whereas the CVD-BN plate with small values of $c_0/2$ was highly oriented [10]. This fact suggests that the geometrical arrangement of BN crystallites also plays an important role in determining the bulk density and internal porosity of CVD-BN plate.

In studying the relationship between the density and the structure of CVD-BN, it will be useful to examine previous studies conducted on carbon materials which have a similar structure to that of boron nitride. In a study on CVD-carbon, Hirai and Yajima [18] have calculated the internal porosity (i.p.) by the following equation: i.p. $= 100\,(d - \varrho)/d$ (%), where ϱ is the observed density and d is the calculated density based on $c_0/2$. The value of i.p. for CVD-carbon varied from a few per cent up to 45% depending on the preparation conditions [18]. It was speculated that the internal pores in CVD-carbon with a large i.p. (45%) were microvoids of about 9 nm diameter, and also pointed out that low-density CVD-carbon had a larger $c_0/2$ value, smaller apparent crystallite size and lower crystallite orientation compared with those of high-density CVD-carbon. From these findings, the models shown in Figs 9a and b were proposed for the arrangement of crystallites in the low- and high-density CVD-carbon, respectively [18]. For glassy carbon, Jenkins *et al.* [19] proposed a fibril structure which consisted of intertwined microfibrils comprising stacks of

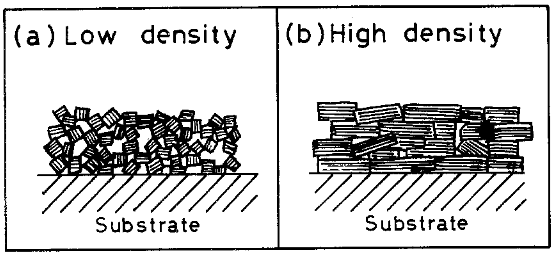

Figure 9 Schematic diagram of configuration of crystallites (after Hirai and Yajima [18]).

narrow graphitic ribbons. Since microvoids are inevitable in the fibril structure, carbon with such a structure has a low density. The structure shown in Fig. 9a may be regarded as a simplified representation of the fibril structure.

The same equation for i.p. was also applied to evaluate the internal porosity of two of the CVD-BN plates prepared in this work, in particular the one with the highest density of 2.14 $\mathrm{g\,cm^{-3}}$ and the other with the lowest density of 1.40 $\mathrm{g\,cm^{-3}}$. The results gave internal porosities of 3.6 and 34%, respectively. The low-density CVD-BN plate ($\varrho = 1.40\,\mathrm{g\,cm^{-3}}$) obtained in the A region had a smaller apparent crystallite size in the *c*-direction (L_c) and showed only a slight crystallite orientation, as compared with the CVD-BN plate formed in the other regions [10]. These features are similar to those of the low-density CVD-carbon. Furthermore, the CVD-BN plate formed in the A region was transparent in spite of its low density, suggesting that its internal pores were in the form of microvoids with diameters of the order of 10 nm, which is similar to that found for CVD-carbon. Therefore, the structure of transparent CVD-BN plate with a low density probably has the arrangement of crystallites as shown in Fig. 9a or possibly the fibril structure.

For the CVD-BN plate formed under 5 torr, the crystallites were highly oriented and the densities were high, even at 1300° C. However, the CVD-BN plates obtained at above 10 torr and a temperature between 1600 and 1800° C had relatively low densities of 1.5 to 1.9 $\mathrm{g\,cm^{-3}}$ (see Fig. 3) despite the fact that their structures showed preferred orientation. These results may be explained in terms of a difference in the formation mechanism of CVD-BN plate. As discussed in the previous paper [10], the formation of t-BN plate at above 10 torr proceeds as follows: cluster (aggregate of polymers) formation in vapour phase → adsorption of cluster on a deposition surface → decomposition of cluster due to heating. When rearrangement and growth of a crystallite (nucleus) adsorbed on the deposition surface do not take place, or when those rates are markedly slower in comparison to the adsorption rates of gaseous intermediates, the structure shown in Fig. 9a is constructed. A cluster, which is an aggregate of polymers, makes little contribution to the growth of a crystallite on the deposition surface. Since rearrangement activity of a crystallite should increase with an increase in T_{dep}, the density of the CVD-BN plate obtained at above 10 torr become influenced by the value of T_{dep}. However, the contribution of rearrangement to densification is rather small, so that the CVD-BN plate formed through the above process has a relatively low density.

Under 5 torr, the CVD-BN plate obtained was composed of two kinds of BN differing in $c_0/2$, and it was suggested that BN with a small $c_0/2$ (t′ or h) is deposited through a different deposition process from that of t-BN formed at above 10 torr [10]. BN crystallites with a small $c_0/2$ are probably formed by the following process: adsorption of gaseous species with low molecular weight on a deposition surface → surface diffusion and growth of crystallite (nucleus). When the growth of crystallite occurs on a deposition surface, CVD-BN plate has a high density because of the filling up microvoids created by rearrangement of crystallites or desorption of product gases. Thus, it can be concluded that for CVD-BN plate obtained at 5 torr the deposition of the BN crystallites having a small interlayer spacing makes a great contribution to the increase in its density.

4.2. Deposition rate

Most of the studies on the synthesis of CVD-BN have had the objective of producing thin films. The rate of increase in thickness reported in these works ranged from a few to several tens of micrometres per hour [2–8]. For free-standing bodies of CVD-BN, Basche [13] reported the rate of increase in thickness of 0.38 $\mathrm{mm\,h^{-1}}$ (unknown conditions for deposition) while Clerc and Gerlach [20] reported 0.4 $\mathrm{mm\,h^{-1}}$ at 1680° C and 1 torr. However, they did not report either structures or densities for the CVD-BN produced at these rates, and thus it is rather difficult to make a detailed comparison with their results and the results obtained in the present experiments.

Malé and Salanoubat [21] investigated the P_{tot} dependence of the deposition rate at 1700° C by using the BCl_3–NH_3 system and reported that the deposition rate was highest at 2 torr. According to Clerc and Gerlach [20], the rate of increase in thickness of CVD-BN formed from the BCl_3–NH_3–H_2–He system reached a maximum at 1 torr. In the present study, on the other hand, the P_{tot} which gave a maximum deposition rate was found to be 20 torr at 1800° C and 30 torr at 1600° C. Though these findings are somewhat inconsistent with the results cited above, both their work and this study found that the deposition rate first increased with an increase in P_{tot} up to its maximum value and then it began to decrease. An increase in P_{tot} leads to an increase in the number of the reactant gas molecules, and as a consequence the deposition will be promoted. A further increase of P_{tot} will initiate homogeneous vapour phase reaction to form a powder product [22]. Thus, a further increase of deposition rate is restrained. The finding that a higher P_{tot} is needed to attain the maximum deposition rate compared to the other past work may be caused by a combination of two facts; first, the present work used a cold-wall CVD apparatus, and secondly it used a gas introduction technique in which BCl_3 and NH_3 were mixed in the very close vicinity of the substrate.

The temperature dependence of the deposition rate constant shown in Fig. 7 is consistent with that of the generally accepted CVD reaction. That is, the rate is controlled by the reaction proceeding on the surface or in the neighbourhood of a substrate in a low-temperature region, and by mass transport in the gas stream in a medium-temperature region. On the other hand, in a high-temperature region the rate is depressed as a result of the formation and growth of homogeneous vapour-phase nuclei [23]. The higher the P_{tot}, the higher the probability of mutual collisions among reactant gas molecules. Consequently, the homogeneous vapour reaction is accelerated even at a relatively low T_{dep}, and the T_{dep} that gives the maximum deposition rate may be lower when P_{tot} is higher as shown in Fig. 7.

For the activation energy of CVD-BN formation, Adams and Capio [8] reported values of 20 to 26 kcal mol^{-1} (84 to 109 kJ mol^{-1}) for the B_2H_6–NH_3–H_2 system at 300 to 340° C, while Nakamura [24] presented the value of 6.3 kcal mol^{-1} (26 kJ mol^{-1}) for the $B_{10}H_{14}$–NH_3 system at 350 to 700° C. There is no known work, however, which deals with activation energy for the BCl_3–NH_3 (H_2) system. A calculation based on the linear portions of the curves in Fig. 7 (1200 to 1400° C under 5 and 10 torr) gave an apparent activation energy of 32 kcal mol^{-1} (134 kJ mol^{-1}). In this region, the rate can be considered to be controlled by the reactions on or near the deposition surface, as previously described. These reactions include adsorption of the reactants onto the deposition surface, their chemical reaction on or near the surface, their surface diffusion, and desorption of the gaseous reaction byproducts. It is also expected that the formation of intermediates, such as BCl_2, $BHCl_2$, BCl [25] and $Cl_3B_3N_3H_3$ [26], and their polymerization, are taking place in the course of the BN formation process from BCl_3 and NH_3. Because of the complex nature of the reactions involved and the lack of data on the bond strength of possible intermediate species, it was difficult to identify the elementary reaction which gave the calculated activation energy of 32 kcal mol^{-1}.

5. Conclusions

1. Various CVD-BN plates having different densities ranging from the maximum of 2.14 to the minimum of 1.40 g cm^{-3} were synthesized in this study. The CVD-BN plate with the maximum density was obtained at a T_{dep} of 2000° C and a P_{tot} of 5 torr.

2. All CVD-BN plates obtained at 5 torr and 1300 to 2000° C had a density above 2.0 g cm^{-3}, and these values showed no dependence on T_{dep}.

3. For the CVD-BN plates formed at above 10 torr, the density increased as T_{dep} was increased.

4. The maximum rate of increase in thickness was 0.4 mm h^{-1} for CVD-BN plates with a high density above 2.0 g cm^{-3}, and 0.6 mm h^{-1} for plates with a density smaller than 2.0 g cm^{-3}.

5. The deposition rate varied with T_{dep} and P_{tot}. The maximum deposition rate showed a different P_{tot} at a different T_{dep}, for example, 20 torr at 1800° C and 30 torr at 1600° C.

6. The apparent activation energy for CVD-BN formation was 32 kcal mol^{-1} (134 kJ mol^{-1}) at 1200 to 1400° C when P_{tot} was 5 or 10 torr.

Acknowledgements

This study was performed under the ERATO Program, promoted by the Science and Technology Agency and the Research Development Corporation of Japan. The authors wish to extend their sincere gratitude to Professor T. Masumoto of the Research Institute for Iron, Steel and Other Metals, Tohoku University, and Director of the Amorphous and Intercalation Compound Project in the ERATO Program, for his never-ending encouragement in pursuit of the present study.

References

1. T. HIRAI, K. NIIHARA and T. GOTO, *J. Mater. Sci.* **12** (1977) 632.
2. M. J. RAND and J. F. ROBERTS, *J. Electrochem. Soc.* **115** (1968) 423.
3. W. BARONIAN, *Mater. Res. Bull.* **7** (1972) 119.
4. M. HIRAYAMA and K. SHONO, *J. Electrochem. Soc.* **122** (1975) 1671.
5. S. B. HYDER and T. O. YEP, *ibid.* **123** (1976) 1721.
6. T. KIMURA, K. YAMAMOTO and S. YUGO, *Jpn J. Appl. Phys.* **17** (1978) 1871.
7. S. P. MURARKA, C. C. CHANG, D. N. K. WANG and T. E. SMITH, *J. Electrochem. Soc.* **126** (1979) 1951.
8. A. C. ADAMS and C. D. CAPIO, *ibid.* **127** (1980) 399.
9. H. MIYAMOTO, M. HIROSE and Y. OSAKA, *Jpn J. Appl. Phys.* **22** (1983) L216.
10. T. MATSUDA, N. UNO, H. NAKAE and T. HIRAI, *J. Mater. Sci.* **21** (1986) 649.
11. J. THOMAS, Jr, M. E. WESTON and T. E. O'CONNOR, *J. Amer. Chem. Soc.* **82** (1962) 4619.
12. R. S. PEASE, *Acta Crystallogr.* **5** (1952) 356.
13. M. BASCHE, US Patent 3 152 006 (1964).
14. N. J. ARCHER, *Spec. Publ. Chem. Soc.* **30** (1977) 167.
15. H. O. PIERSON, *J. Compos. Mater.* **9** (1975) 228.
16. J. ECONOMY and R. V. ANDERSON, *J. Polym. Sci. C* 19 (1967) 283.
17. B. E. WARREN, *Phys. Rev.* **59** (1941) 693.
18. T. HIRAI and S. YAJIMA, *J. Mater. Sci.* **2** (1967) 18.
19. G. M. JENKINS, K. KAWAMURA and L. L. BAN, *Proc. R. Soc.* **A327** (1972) 501.
20. G. CLERC and P. GERLACH, in Proceedings of 5th International Conference on Chemical Vapor Deposition, edited by J. M. Blocher, Jr, H. E. Hintermann and L. H. Hall (Electrochemical Society, Princeton, 1975) p. 777.
21. G. MALÉ and D. SALANOUBAT, in Proceedings of 7th International Conference on Chemical Vapor Deposition, edited by T. O. Sedgwick and H. Lydtin (Electrochemical Society, Princeton, 1979) p. 391.
22. J. M. BLOCHER, Jr, *J. Vac. Technol.* **11** (1974) 680.
23. W. A. BRYANT, *J. Mater. Sci.* **12** (1977) 1285.
24. K. NAKAMURA, *J. Electrochem. Soc.* **132** (1985) 1757.
25. H. HANNACHE, R. NASLAIN and C. BERNARD, *J. Less-Common Metals* **95** (1983) 221.
26. L. E. BRANOVICH, M. L. LONG and W. B. P. FITZPATRICK, AD Report 733292 (1971).

Received 16 February
and accepted 28 April 1987